The functional significance of EEG microstates—Associations with modalities of thinking

P. Milz [a,*], P.L. Faber [a], D. Lehmann [a,1], T. Koenig [b], K. Kochi [a], R.D. Pascual-Marqui [a]

[a] The KEY Institute for Brain-Mind Research, Department of Psychiatry, Psychotherapy and Psychosomatics, University Hospital of Psychiatry, P.O. Box 1931, CH-8032 Zurich, Switzerland
[b] Department of Psychiatric Neurophysiology, University Hospital of Psychiatry, University of Bern, Bern, Switzerland

ARTICLE INFO

ABSTRACT

The momentary, global functional state of the brain is reflected by its electric field configuration. Cluster analytical approaches consistently extracted four head-surface brain electric field configurations that optimally explain the variance of their changes across time in spontaneous EEG recordings. These four configurations are referred to as EEG microstate classes A, B, C, and D and have been associated with verbal/phonological, visual, attention reorientation, and subjective interoceptive-autonomic processing, respectively. The present study tested these associations via an intra-individual and inter-individual analysis approach. The intra-individual approach tested the effect of task-induced increased modality-specific processing on EEG microstate parameters. The inter-individual approach tested the effect of personal modality-specific parameters on EEG microstate parameters. We obtained multichannel EEG from 61 healthy, right-handed, male students during four eyes-closed conditions: object-visualization, spatial-visualization, verbalization (6 runs each), and resting (7 runs). After each run, we assessed participants' degrees of object-visual, spatial-visual, and verbal thinking using subjective reports. Before and after the recording, we assessed modality-specific cognitive abilities and styles using nine cognitive tests and two questionnaires. The EEG of all participants, conditions, and runs was clustered into four classes of EEG microstates (A, B, C, and D). RMANOVAs, ANOVAs and post-hoc paired t-tests compared microstate parameters between conditions. TANOVAs compared microstate class topographies between conditions. Differences were localized using eLORETA. Pearson correlations assessed interrelationships between personal modality-specific parameters and EEG microstate parameters during no-task resting.

As hypothesized, verbal as opposed to visual conditions consistently affected the duration, occurrence, and coverage of microstate classes A and B. Contrary to associations suggested by previous reports, parameters were increased for class A during visualization, and class B during verbalization. In line with previous reports, microstate D parameters were increased during no-task resting compared to the three internal, goal-directed tasks. Topographic differences between conditions concerned particular sub-regions of components of the metabolic default mode network. Modality-specific personal parameters did not consistently correlate with microstate parameters except verbal cognitive style which correlated negatively with microstate class A duration and positively with class C occurrence.

This is the first study that aimed to induce EEG microstate class parameter changes based on their hypothesized functional significance. Beyond, the associations of microstate classes A and B with visual and verbal processing, respectively and microstate class D with interoceptive-autonomic processing, our results suggest that a finely-tuned interplay between all four EEG microstate classes is necessary for the continuous formation of visual and verbal thoughts, as well as interoceptive-autonomic processing. Our results point to the possibility that the EEG microstate classes may represent the head-surface measured activity of intra-cortical sources primarily exhibiting inhibitory functions. However, additional studies are needed to verify and elaborate on this hypothesis.

* Corresponding author at: The KEY Institute for Brain-Mind Research, University Hospital of Psychiatry, P.O. Box 1931, CH-8032 Zurich, Switzerland.
E-mail addresses: patricia.milz@key.uzh.ch (P. Milz), pfaber@key.uzh.ch (P.L. Faber), dlehmann@key.uzh.ch (D. Lehmann), thomas.koenig@puk.unibe.ch (T. Koenig), osakachochiku@gmail.com (K. Kochi), pascualm@key.uzh.ch (R.D. Pascual-Marqui).
[1] Deceased.

Introduction

The momentary, global functional state of the brain is reflected by its electric field configuration. The time-course of brain electric field configurations can be analyzed with high resolution, "millisecond by millisecond" using head-surface EEG recordings (Koenig et al., 2002). Inspecting these time-courses reveals that these electric field configurations

change discontinuously, i.e. particular configurations remain quasi-stable for a duration of approximately 100 ms and then transition abruptly to another configuration (Lehmann et al., 1987, 2009; Michel et al., 2009). Cluster analytical approaches consistently extracted four head-surface brain electric field configurations that explain approximately 80% of the variance of these changes across time in spontaneous EEG recordings (Koenig et al., 2002; Wackermann et al., 1993). These four states are referred to as EEG microstate classes and are conventionally labeled from A through D (Koenig et al., 2002). The particular instances of these four states as quasi-stable configurations observed over the time-course of brain electric field configuration changes are referred to as "brain electric microstates" (Lehmann, 1990). The previous literature suggests that these brain electric microstates qualify as basic building blocks of mentation and may be considered candidates for conscious or non-conscious "atoms of thought and emotion" (Lehmann, 1990; Lehmann et al., 2004, 2005; Lehmann and Michel, 2011; Strik et al., 1998).

Changes in topography, and other parameters such as mean duration, occurrence, coverage, and syntax (microstate sequence) of the four EEG microstate classes have been reported across stages of development (Koenig et al., 2002), in psychopathology compared to health (disorders of consciousness: Fingelkurts et al., 2012; schizophrenia: Andreou et al., 2014; Kikuchi et al., 2007; Kindler et al., 2011; Koenig et al., 1999; Lehmann et al., 2005; Nishida et al., 2013; Strelets et al., 2003; Tomescu et al., 2014, 2015; depression: Strik et al., 1995; dementia: Strik et al., 1997), in states of sleep (Brodbeck et al., 2012; Wehrle et al., 2007), in altered states such as hypnosis (Katayama et al., 2007) and meditation (Faber et al., 2005, 2014), and for particular personality profiles compared to others (Schlegel et al., 2012).

Despite the obvious need to understand the functional significance of these four EEG microstate classes to interpret the above changes, the functional significance of these four EEG microstate classes was only directly targeted in very few studies.

Britz et al. (2010) carried out a simultaneous EEG–fMRI study where the four EEG microstate classes were spatially correlated with four of the fMRI resting-state networks that had previously been attributed to phonological processing (microstate class A), visual imagery (microstate class B), attention reorientation (microstate class C), and subjective interoceptive-autonomic processing (microstate class D). Associations of EEG microstates with visual as opposed to non-visual processing are also supported by reports that showed different microstate topographies for visual as opposed to abstract thoughts (Koenig et al., 1998; Lehmann et al., 1998, 2010).

However, a more recent study suggested that the four EEG microstate classes may reflect the temporally distinct electrophysiological activation of four main components of the default mode network (Pascual-Marqui et al., 2014). The correspondence of the intra-cortical sources of the four EEG microstate classes with the four main components of the default mode network suggests that the metabolic DMN as measured with fMRI may reflect a time averaged version of distinct electrical networks which only become identifiable with the increased time resolution available in EEG recordings. An increase of metabolic DMN activity is associated with no-task resting, as well as a wide range of internal, goal-directed tasks (Andrews-Hanna, 2012). Possibly, the increased time resolution of the EEG will allow us to obtain a more detailed account of the roles of the four temporally distinct electrophysiological DMN components by assessing the effects of internal, goal-directed tasks as compared to no-task resting on the four EEG microstate classes.

The present study used four conditions, three internal, goal-directed tasks (object-visualization, spatial-visualization, verbalization) and no-task resting, to induce increased visual, verbal, and subjective interoceptive-autonomic processing, respectively. Subjective reports after conditions assessed participants' degree of object-visual, spatial-visual, and verbal thinking; cognitive tests assessed participants' object-visual, spatial-visual, and verbal abilities; and cognitive style questionnaires assessed participants' object-visual, spatial-visual, and verbal cognitive style. An intra-individual analysis approach tested the success of the induction of the particular thinking modality, and the effects of the four conditions on the occurrence, duration, coverage, and topography of the four EEG microstate classes. An inter-individual analysis approach correlated EEG microstate parameters during resting with the subjective degree of modality-specific thinking, as well as modality-specific cognitive abilities and style.

Firstly, we expected intra-individual differences between conditions in the degree of subjectively reported thinking modality and EEG microstate properties (occurrence, duration, coverage, and topography). Secondly, we expected inter-individual differences reflected by correlations of the degree of subjectively reported thinking modality, modality-specific cognitive abilities, and style with EEG microstate parameters (occurrence, duration, coverage) during resting. Thirdly, we expected correspondences between these intra- and inter-individual differences.

Methods

Participants

Seventy healthy right-handed male volunteers from the University of Zurich and the Swiss Federal Institute of Technology Zurich were invited via flyers and through the Participant Server of the Institute of Psychology of the University of Zurich. Applicants were screened with an online questionnaire and excluded when they reported a history of head trauma, brain disease, or current drug usage. The first 70 qualifying men were invited to participate in the EEG experiment. Only male participants were considered because of the effects of the menstrual cycle and hormonal contraceptives on EEG in women (Becker et al., 1982; Krug et al., 1999). Each participant received 40 Swiss Francs for their participation. The Ethics Committee of the Canton of Zurich approved the experimental protocol (reference number: KEK-ZH-Nr. 2011-0278). All participants gave their written informed consent. After EEG pre-processing, EEG data from 61 participants was available (mean age 24.2 years, SD = 3.3, range = 18–34). Behavioral data were available for 60 of these 61 participants. All of these participants were right-handed (German version of the Edinburgh handedness inventory by Oldfield, 1971: mean = 4.48, SD = 0.38 where 1 indicates left-handedness and 5 right-handedness). The reasons for participant rejection are listed in the data pre-processing section.

Questionnaires

Modality of Thinking Questionnaire (MOTQ)

The MOTQ (Milz et al., submitted for publication) is a self-rating questionnaire based on the object-spatial–verbal cognitive style model (Blazhenkova and Kozhevnikov, 2009). It assesses modality-specific cognitive style in three dimensions: object-visualization, spatial-visualization, and verbalization. It comprises 36 items: 12 items to assess each style dimension. Each item asks respondents to rate their degree of agreement with a modality-specific statement on a 5-point Likert-scale ranging from 1 (*complete disagreement*) to 5 (*absolute agreement*). Participants' scores were obtained separately for each dimension by computing the mean of the items of the respective scale. The reliabilities of the three scales are high (internal consistency: 0.81–0.86; re-test reliability: 0.85–0.87; Milz et al., submitted for publication).

Cognitive tests

Object-visual ability

To assess object-visual ability, we used the Snowy Pictures Test Part 1 and 2 (Ekstrom et al., 1976), and the Incomplete Pictures Test (Horn, 1962). The former two ask participants to identify objects hidden in

an image of short unconnected lines (3 min time for twelve images each). The latter asks participants to identify the first letter of the name of small images of incomplete drawings of objects from a selection of five letters (one minute time for 40 images). Each correctly identified solution was added up to retrieve a sum score for each of the three tests.

Spatial-visual ability

To assess spatial-visual ability, we used the Paper Folding Test Part 1 and 2 (PFT: Ekstrom et al., 1976), and the "Cube Test" (Wuerfelabwicklungen: Meili, 1955). The former ask participants to identify an unfolded paper which had previously been folded in a series of steps and then punched, by its holes from a selection of five solutions (3 min time for ten images each). The latter asks participants to label top and connecting edges of unfolded cubes by imagining what they would look like if folded (10 min time for eleven images). Each correctly identified solution was added up to retrieve a sum score for each of the three tests.

Verbal ability

To assess verbal ability, we used the Masselon, Part–Whole, and the Insight Test from the verbal dimension of the Berlin Intelligence Structure Test (Jäger et al., 1997). The Masselon Test asks participants to write down as many sentences possible containing three defined nouns (two min time), the Part–Whole Test asks participants to identify wholes if they are followed by their part (e.g. "year" if followed by "month") in four columns of nouns (40 s time). The Insight Test asks participants to write down as many keywords possible to explain a given statement (e.g. why to a person fashion may be important) (2 min time). Correct sentences for the Masselon Test, correctly identified wholes for the Part–Whole Test, and reasonable keywords for the Insight Test were added up to retrieve a sum score for each of the three tests.

Recording

EEG recordings were done at the KEY Brain Mapping Laboratory at the University Hospital of Psychiatry, Zurich, using a 64-channel BioSemi Recording System. Sixty-four electrodes were attached using a Biosemi Headcap at the following positions: Fp1/2, Fpz, AF7/8, AF3/4, AFz, F7/8, F5/6, F3/4, F1/2, Fz, FT7/8, FC5/6, FC3/4, FC1/2, FCz, T7/8, C5/6, C3/4, C1/2, Cz, TP7/8, CP5/6, CP3/4, CP1/2, CPz, P7/8, P5/6, P3/4, P1/2, Pz, PO7/8, PO3/4, POz, O1/2, Oz, P9/10, and Iz (according to the International "10-10 System", Chatrian et al., 1985; Nuwer, 1987). Eye movements were tracked using 2 additional electrodes, one above the left and one below the right eye. Breathing was recorded with a strain gauge chest band. Recordings were done with a sampling frequency of 2048 Hz.

Protocol

Prior to the experiment, participants completed an online version of the Modality of Thinking Questionnaire (MOTQ: Milz et al., submitted for publication) and the Vividness of Visual Imagery Questionnaire (VVIQ: Marks, 1973). On arrival at the EEG laboratory, participants were informed and gave their consent to their participation in the experiment. Then, they completed the Edinburgh handedness test (Oldfield, 1971) and a computerized version of the Object-Spatial Imagery and Verbal Questionnaire (OSIVQ: Blazhenkova and Kozhevnikov, 2009, purchased via MM Virtual Design). During electrode attachment, the experimental design and the upcoming tasks were thoroughly explained and participants were informed that during each of the upcoming recording runs they should sit relaxed with arms and legs in a comfortable position. Participants were then seated in an electrically, acoustically and light-shielded chamber on an armchair, viewing a computer monitor at 1 m. Each participant was recorded during four eyes-closed conditions: no-task resting (7 recording runs), object-visualization, spatial-visualization, and verbalization (6 recording runs each). Each recording run lasted 50 s and conditions were presented in pseudo-randomized order (no-task resting always initiated a permutation of the other three tasks, and ended the recording).

Instructions were again presented on the monitor prior to each run using Presentation® (www.neurobs.com). Before no-task resting runs, participants were asked to just relax and close their eyes until a tone would indicate the end of that run. Before visualization runs, participants were asked to memorize an upcoming image and to then visualize it internally with their eyes closed for the whole period of the 50 s recording. The image was visible for 7 s. For the six object-visual runs, images were six photos containing many visual details such as colors, textures, and shapes (objects were foods: apple bowl, bread loaf; furniture: bed, lamp; and animals: deer, tigers). For the six spatial-visual runs, images were six spatial configurations of black circles. Before verbalization runs, participants were asked to read an upcoming noun to then think of a verbal definition for that noun to internally explain its meaning to an imaginary other person. The noun was visible for 2 s. For the six verbalization runs, six nouns of lowest visually imaginable ranking according to Baschek et al. (1977) were displayed. Stimulus examples are illustrated in Fig. 1.

After each run, participants reported their degree of object-visual, spatial-visual, and verbal thinking during task execution by specifying their agreement to three corresponding statements (for object-visual: "My thinking was comprised of concrete, detailed, realistic visual images."; for spatial-visual: "My thinking was comprised of images depicting spatial relations between objects."; for verbal: "My thinking was very verbal in nature.") on a continuous rating scale ranging from 0 (*not at all*) to 100 (*very much so*). Moreover, for object-visual tasks, they answered a three-option multiple choice question regarding the photography they had perceived (e.g. "How were the dots on the deer aligned?"). For the spatial-visual tasks, they chose the spatial configuration they had just visualized from three possible configurations (only one of which was correct). For the verbalization task, participants entered their definition within 30 s using a keyboard on a table in front of them.

It was emphasized to participants that their success in answering these questions and the quality of their definition was of minor

| Object-Visualization | Spatial-Visualization | Verbalization |
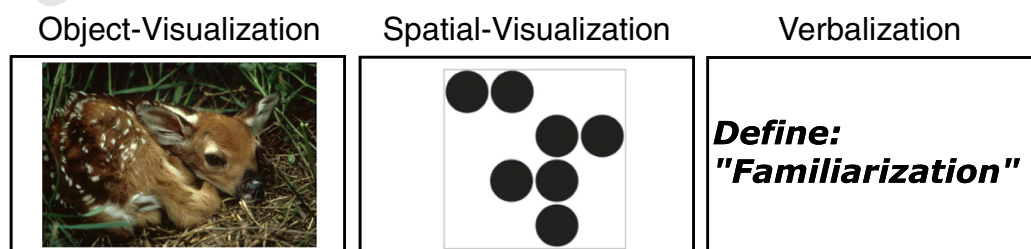
Fig. 1. Example stimuli for the three tasks: object-visualization, spatial-visualization, and verbalization. Image source for the object-visualization example: http://www.public-domain-image.com/fauna-animals-public-domain-images-pictures/deers-public-domain-images-pictures/white-tailed-deer-pictures/white-tailed-deer-fawn-in-grass-odocoileus-virginianus.jpg.html.

importance. Instead, their main focus should be to visualize as well as possible during the visualization tasks and to verbalize as well as possible during the verbalization task. Regarding their answer to the degree of object-visual, spatial-visual, and verbal thinking during tasks, they were told that it would be best for the experiment if they answered as truthfully as possible even if their thinking may not have been in line with what they had been asked to do. After the EEG recording, participants' abilities in the three thinking modalities were assessed using three cognitive tasks each for object-, spatial- visual, and verbal ability. Two weeks after the experiment, participants completed the MOTQ and OSIVQ a second time.

The answers to multiple choice questions after the visualization runs and the definitions written after the verbalization runs clearly indicated that participants had successfully remembered the images they had perceived ($88.4 \pm 9.35\%$ correct answers) and were able to form a definition within the given time period. Of the 61 participants, 59 were able to form a coherent definition (sometimes simply not yet complete) across the six runs as assessed by two independent raters.

Data pre-processing

EEG data were pre-processed using Brain Vision Analyzer 2 (Brain Products, Munich, Germany). Eye movement artifacts were removed using the software's ocular correction ICA. Sweat, muscle, movement, and electrode artifacts were discarded through visual inspection. Channels with severe artifacts across the whole recording run (mean number of channels across participants = 6.7, SD = 3.8) were interpolated. Interpolations were done separately for each affected run. All channels directly surrounding the affected channel were used for interpolation unless they were contaminated with severe artifacts themselves. Three channels (P9, P10, and Iz) were discarded for the analysis because they were spatial outliers relative to the other 61 electrodes that cover the scalp in an approximate uniformly distributed manner (see also: Pascual-Marqui et al., 2014). The data was then segmented into 2-s epochs, down-sampled to 256 Hz, re-referenced to average reference, and FFT filtered from 2–20 Hz (no windowing). After data conditioning, the mean number of available data epochs per run (average across the 25 runs: 6 runs each for object-visualization, spatial-visualization, and verbalization, 7 runs for resting) ranged between 3.36 and 21.76 (S.D. between 2.48 and 6.56) across participants. On average, 12.88 epochs (SD = 4.14) were available for each participant in each run. The EEG of five participants had to be rejected because of strong eye rolling artifacts across the whole recording which could not be satisfactorily removed with ocular correction ICA approaches. Another four participants had to be rejected because of severe local frontal and temporal muscular artifacts across the whole recording which could not be satisfactorily compensated for with interpolation procedures since they affected up to eight surrounding channels. Due to technical problems with the Presentation software, behavioral data for one participant were not available.

Microstate analysis

Microstate class computation

The microstate class computations were done following the procedure described in (Koenig et al., 1999) using the implementation in the microstate package of the KEY EEG Python library (Milz, in preparation). This open source library provides EEG pre-processing and analysis routines implemented in the Python programming language. For each participant, each condition, and each run, the EEG map topographies at time points of global field power peaks (GFPL1 Norm: Lehmann and Skrandies, 1980) were collected and fed into a modified k-means clustering algorithm (see also Pascual-Marqui et al., 1995) to deduce the four classes of map topographies that maximally explain the variance of the map topographies (see also Koenig et al., 1999; Koenig et al., 2002). These four classes of map topographies were then used to compute *mean classes* across runs, which were then used to compute mean classes across participants, which were finally used to compute mean classes across conditions. The following description depicts how the mean classes across runs were computed. However, we applied the same procedure to compute mean classes across participants, and across conditions, thereafter. Mean classes across runs were computed by using a full permutation procedure that determines the solution of maximal mean correlation across the four classes across all runs. The means across runs were computed as the first principle component of all maps that were assigned to each other in this solution.

Microstate parameter computation

Using the mean microstate classes across conditions as templates, for all participants, all conditions, all runs, and each two-second epoch, the EEG map topographies at global field power peaks were assigned to one of these 4 microstate classes based on maximal Pearson correlation. Successive GFP peak maps (*maps*) assigned to the same class were recognized as belonging to one *microstate*. The duration of a microstate was computed as the time period during which maps were successively assigned to the same class, starting at the midpoint between the last map of the preceding microstate and the first map of the following microstate. Based on a given 2-s epoch, we cannot reconstruct when the first microstate began (previous epoch) and when the last microstate ended (next epoch). Therefore, their duration cannot conclusively be determined. For this reason, the first and last microstate of each 2-s epoch were ignored for the following parameter computations.

Three microstate parameters were computed: *mean duration* (average time in ms covered by a given microstate class), *occurrence* (mean number of distinct microstates of a given class occurring within a 1 s window), and *coverage* (percentage of time covered by a given microstate class). Computations were done for each participant, each condition, each run, and each microstate class by averaging the respective parameter values across all 2-s epochs of a given run (see also Strelets et al., 2003).

Analysis methods

Intra-individual analysis

Where not otherwise specified, statistics were computed using SPSS Version 22.0 (IBM Corporation, 2014).

Success of modality induction. Subjective reports on the degree of object-visual, spatial-visual, and verbal thinking during the four conditions were averaged across repeated runs. A repeated measures MANOVA (independent variable: condition, dependent variable: degree of object-visual thinking, spatial-visual thinking, and verbal thinking), post-hoc ANOVAs, and paired *t*-tests tested whether the three tasks induced thinking in the attempted modality.

Mauchly's Test of Sphericity indicated that the assumption of sphericity had been violated for object-visual thinking ($\chi^2(5) = 24.65$, $p = 0.0001$), spatial-visual thinking ($\chi^2(5) = 19.47$, $p = 0.0016$), and verbal thinking ($\chi^2(5) = 20.24$, $p = 0.0011$). Therefore, results are reported with Greenhouse–Geisser correction.

Task effects on microstate parameters. Microstate duration, occurrence, and coverage during the four conditions were averaged across repeated runs. For each microstate parameter (duration, occurrence, and coverage), a repeated measures MANOVA (independent variable: condition, dependent variable: parameter values of classes A, B, C, D), post-hoc ANOVAs and paired *t*-tests tested whether the three tasks affected the three microstate parameters.

Mauchly's Test of Sphericity indicated that the assumption of sphericity had been violated for duration, occurrence, and coverage for all four EEG microstate classes ($\chi^2(5) > 11.91$, $p < 0.05$). Therefore, results are reported with Greenhouse–Geisser correction.
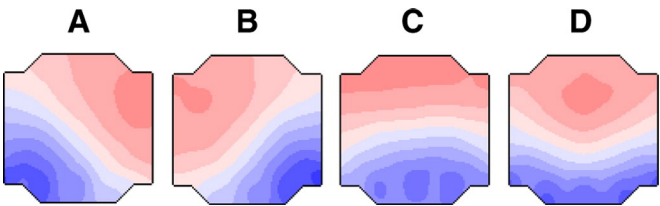
Fig. 2. The topographies of the four microstate classes retrieved from the clustering algorithm, sorted and labeled according to the normative classes described in Koenig et al. (2002). Note that only the map's topography is important, whereas polarity is disregarded in the spontaneous EEG clustering algorithm.

Task effects on microstate topographies. The EEG map topographies of the four classes for the four conditions were tested for global differences using TANOVA (Strik et al., 1998) implemented in RAGU (Koenig et al., 2011). TANOVA computes the Global Map Dissimilarity (Lehmann and Skrandies, 1980) between two map topographies and the probability of the observed differences using a randomization procedure. In a first step, a two-factor TANOVA (independent variables: class, condition; dependent variable: map topography) was computed. In a second step, class-wise one-factor TANOVAs (independent variable: condition; dependent variable: map topography) were computed. Channel-wise paired *t*-tests specified the spatial distribution of observed differences. The intra-cortical sources of significant differences were localized using exact low resolution electromagnetic tomography (eLORETA: Pascual-Marqui, 2007).

Inter-individual analysis

Correlations between microstate parameters across conditions. We computed Pearson correlations between the microstate parameters of the four conditions (object-visualization, spatial-visualization, verbalization, and no-task resting) for each condition pair (means across runs).

Correlations between microstate parameters and subjectively reported thinking modality. We computed Pearson correlations between the

Table 1
Multivariate effects of condition on self-reported degree of thinking in the three modalities (object-visual, spatial-visual, and verbal).

Dependent variable	df	df error	F	p	Wilks' Λ	Partial η²
Degree of thinking	9	51	100.362	<0.001	0.053	0.95

duration, occurrence, and coverage of the four EEG microstate classes and the reported degree of object-visual, spatial-visual, and verbal thinking during resting (means across runs, and separately for each resting run).

Correlations between microstate parameters and modality-specific ability. We computed Pearson correlations between modality-specific abilities and the duration, occurrence, and coverage of the four EEG microstate classes during resting (means across runs). Correlations were computed separately for an object-visual, spatial-visual, and verbal ability factor derived from a principal component analysis of the nine cognitive tests (see Inline Supplementary Table S1).

Inline Supplementary Table S1 can be found online at http://dx.doi.org/10.1016/j.neuroimage.2015.08.023.

Correlations between microstate parameters and modality-specific style. **Q3** We computed Pearson correlations between modality-specific cognitive style and the duration, occurrence, and coverage of the four EEG microstate classes during resting (means across runs). Correlations were computed separately for object-visual, spatial-visual, and verbal style based on the MOTQ (means across the two assessment time points).

Results

Microstate classes

Across participants, the topographies of the individual four microstate classes explained 84.0 ± 4.8% of the total variance of all GFP peaks, and 77.0 ± 5.1% of the variance of all EEG time frames. The four mean microstate classes across conditions are illustrated in Fig. 2. The
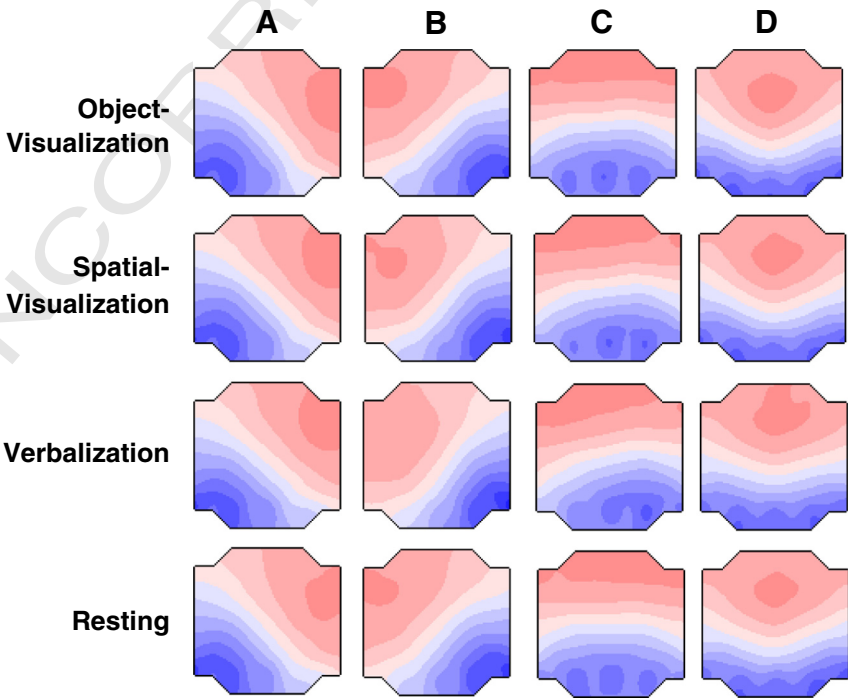
Fig. 3. The four microstate classes retrieved from the clustering algorithm for the four conditions (object-visualization, spatial-visualization, verbalization, and no-task resting) separately. They were sorted and labeled according to the normative classes described in Koenig et al. (2002).

Table 2
Univariate effects of condition on self-reported degree of object-visual, spatial-visual, and verbal thinking (values based on Greenhouse–Geisser correction).

Dependent variable	df	df error	F	p	Partial η²
Object-visual thinking	2	136	87.922	<0.001	0.60
Spatial-visual thinking	3	149	319.619	<0.001	0.84
Verbal thinking	3	150	172.594	<0.001	0.75

Table 3
Multivariate effects of condition on duration, occurrence, and coverage of the four microstate classes A, B, C, and D.

Dependent variable	df	df error	F	p	Wilks' Λ	Partial η²
Duration	12	49	2.734	0.007	0.599	0.40
Occurrence	12	49	3.126	0.002	0.566	0.43
Coverage	12	49	3.914	<0.001	0.511	0.49

four mean microstate classes across participants, separately for the four conditions are illustrated in Fig. 3. The topographies were labeled as classes A, B, C, and D based on their best fit with the four normative classes described in Koenig et al. (2002).

Intra-individual analysis

Success of modality induction

Analyses of variance revealed a significant effect of condition on object-visual, spatial-visual, and verbal thinking (Tables 1, 2). The self-reported degrees of object-visual, spatial-visual, and verbal thinking during the four conditions are illustrated in Fig. 4. Post-hoc *t*-tests revealed that during each task (object-visualization, spatial-visualization, and verbalization) participants were thinking more strongly in the modality that was attempted to be induced than in other modalities (Inline Supplementary Table S2). Moreover, they were thinking most strongly in the modality that was attempted to be induced in the task which attempted to induce it compared to the other tasks and also compared to resting (Inline Supplementary Table S3). This was true for all three tasks but most prominent for the verbalization task (see Fig. 4).

Inline Supplementary Tables S2 and S3 can be found online at http://dx.doi.org/10.1016/j.neuroimage.2015.08.023.

Task effects on EEG microstate parameters

Analyses of variance revealed a significant effect of condition on microstate duration, occurrence, and coverage for microstate classes A and B (Tables 3 and 4).

Post-hoc paired *t*-tests revealed a similar pattern of differences between conditions for the three parameters (Inline Supplementary Tables S4–S7).

Inline Supplementary Tables S4–S7 can be found online at http://dx.doi.org/10.1016/j.neuroimage.2015.08.023.

Table 5 illustrates all significant differences ($p < 0.05$) and trends ($p < 0.10$). For microstate class A, parameters were increased during the visualization compared to the other conditions. For microstate class B, parameters were increased during the verbalization compared to the other conditions. Microstate class C was shorter during visualization compared to resting. Microstate class D lasted longer during resting compared to verbalization, occurred more often during resting compared to visualization, and showed increased coverage compared to both object-visualization and verbalization. There were no significant differences between the two visualization tasks.

Fig. 5 illustrates the absolute magnitude of coverage (in percent) observed for the four microstate classes. We note lower mean coverage (20–24%) for microstate classes A and B as compared to microstate classes C and D (27–30%) during all conditions. The absolute magnitude of significant ($p < 0.05$) coverage differences between conditions for
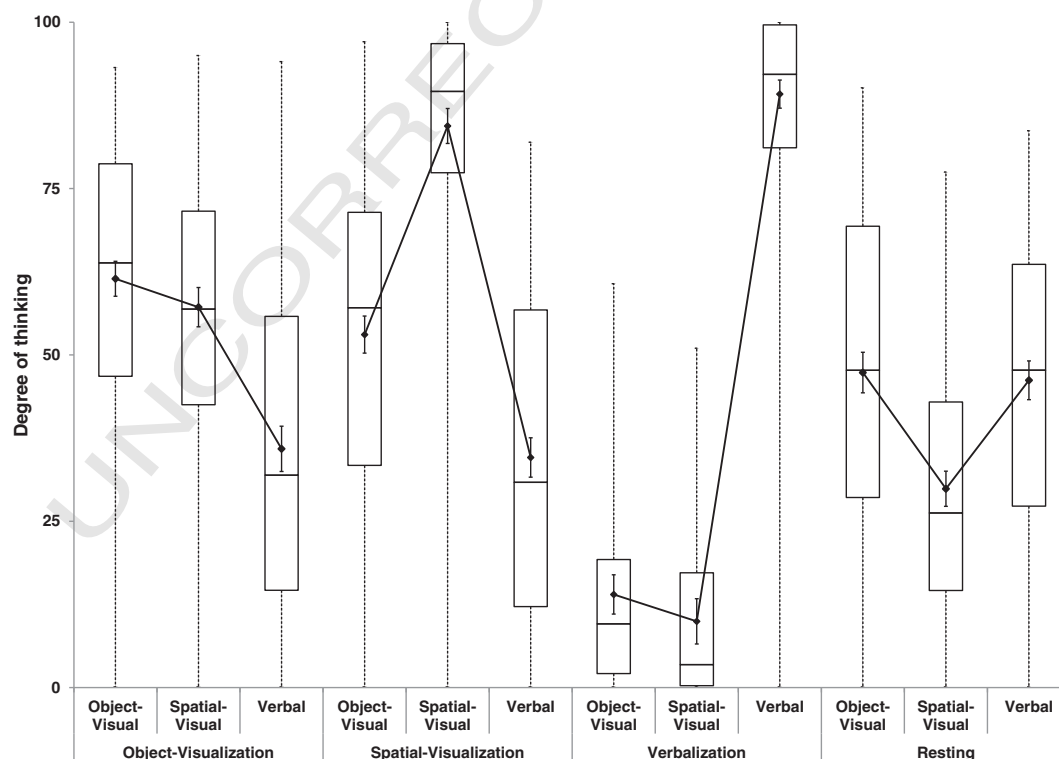
Fig. 4. Self-reported degree of object-visual, spatial-visual, and verbal thinking during the three tasks (object-visualization, spatial-visualization, and verbalization) and during no-task resting. The end of the lower whisker of the boxes represents the minima, the boxes lower bound the first quartiles, the midline the medians, the boxes upper bound the third quartiles, and the end of the upper whisker the maxima of the distributions of participants' degree of thinking modality, respectively. Distribution means are indicated by the small circles within the boxes, standard errors are indicated by the error bars starting from these circles. The means are connected with lines within each condition ($N = 60$).

Table 4

Univariate effects of condition on duration, occurrence, and coverage of the four micro-state classes A, B, C, and D (Greenhouse–Geisser corrected values).

Dependent variable		df	df error	F	p	Partial η^2
Duration	A	2.5	151	4.164	0.011	0.06
	B	2.1	128	7.020	0.001	0.10
	C	1.7	102	1.923	0.157	0.03
	D	2.4	144	1.200	0.309	0.02
Occurrence	A	2.7	160	7.510	<0.001	0.11
	B	2.4	143	5.172	0.004	0.08
	C	2.2	134	0.103	0.920	0.00
	D	2.6	156	1.940	0.134	0.03
Coverage	A	2.5	147	11.432	<0.001	0.16
	B	2.1	125	10.518	<0.001	0.15
	C	2.2	132	0.442	0.663	0.01
	D	2.3	139	2.092	0.120	0.03

Table 5

Microstate parameter changes between the four conditions: resting (Re), object-visualization (Ov), spatial-visualization (Sv), and verbalization (Ve).

Conditions	Duration				Occurrence				Coverage			
	A	B	C	D	A	B	C	D	A	B	C	D
Ov → Ve	↘	↗			↘	↗			↘	↗		
Sv → Ve	↘	↗			↘	↗			↘	↗		
Ov → Sv												
Re → Ov	↗		↘		↗		↘					↘
Re → Sv			↘		↗		↘			↗		
Re → Ve	↗		↘		↗				↘	↗		↘

Differences at $p < 0.10$ are depicted by arrows; arrows for $p < 0.05$ are in bold (no correction for multiple testing).

Table 6

Paired TANOVA p-values for each condition pair.

Conditions			Microstate classes			
			A	B	C	D
Ov	–	Ve	*__0.048__*	<*__0.001__*	<*__0.001__*	<*__0.001__*
Sv	–	Ve	0.407	0.177	*__0.013__*	*__0.004__*
Ov	–	Sv	0.202	*__0.015__*	0.125	0.482
Re	–	Ov	0.145	0.593	0.165	0.096
Re	–	Sv	0.485	0.098	*__0.004__*	0.100
Re	–	Ve	0.415	*__0.003__*	<*__0.001__*	*__0.002__*

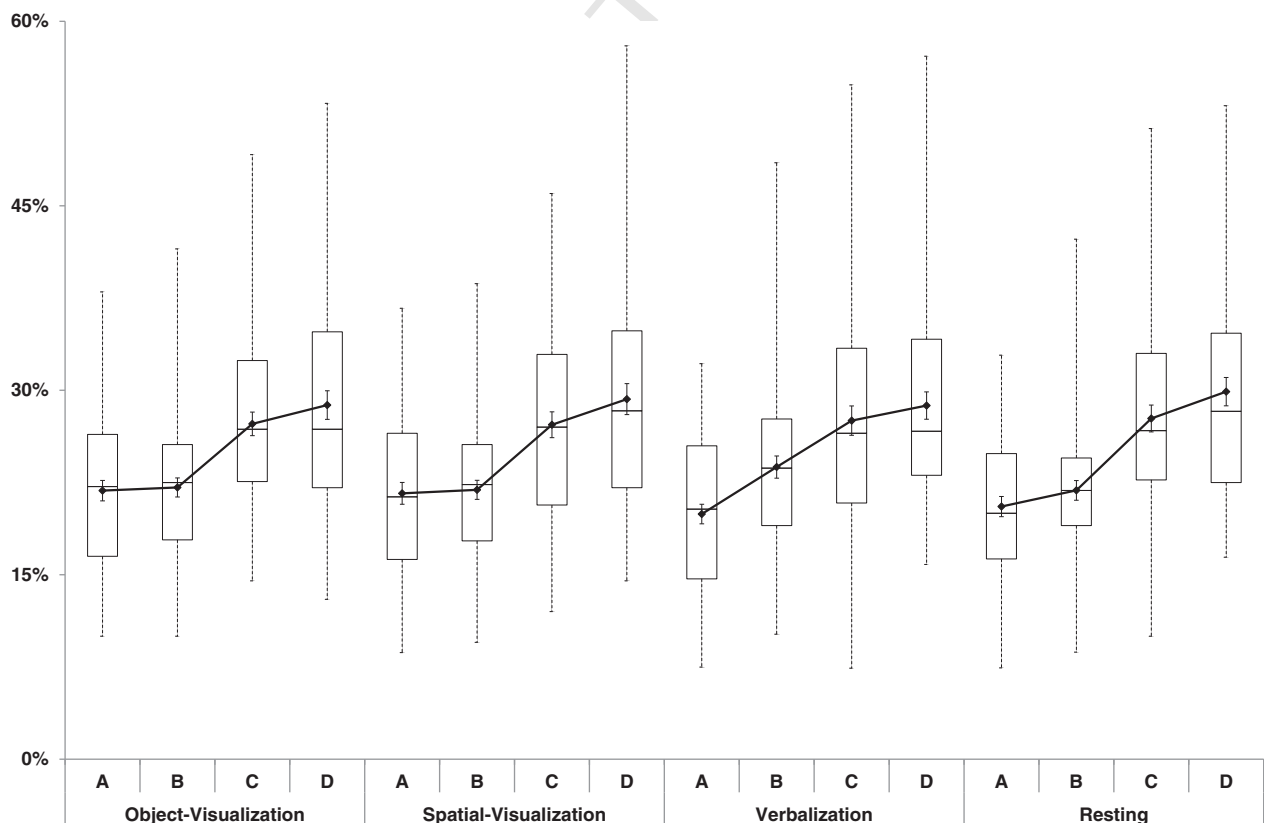Re: resting, Ov: object-visualization, Sv: spatial-visualization, Ve: verbalization.
Significant differences ($p < 0.05$, no cmt) are bold, italic, and underlined.

microstate classes A and B was of moderate effect size (absolute effect sizes ranging from 0.38 to 0.60, see also Inline Supplementary Table S7).

Task effects on EEG microstate topographies

The two-factor TANOVA revealed a significant effect of microstate class ($p < 0.001$) and the interaction between condition and microstate class ($p < 0.001$) on microstate map topographies. Separate one-factor TANOVAs for the four EEG microstate classes revealed a significant effect of condition on microstate map topographies for Map B ($p < 0.001$), Map C ($p < 0.001$), and Map D ($p < 0.001$). Post-hoc paired TANOVAs revealed significant topographic differences between several condition pairs (see Table 6). Topographic differences of these significant differences are illustrated in Fig. 6.

Multidimensional scaling (Koenig et al., 2011) of the maps for all four conditions revealed that object- and spatial-visualization deviated similarly from verbalization on the left–right and anterior–posterior map topography for microstate classes C and D, respectively. Moreover,

Fig. 5. Box-plots illustrating the coverage of the four microstate classes A, B, C, and D during the four conditions (object-visualization, spatial-visualization, verbalization, and no-task resting). The end of the lower whisker of the boxes represents the minima, the boxes lower bound the first quartiles, the midline the medians, the boxes upper bound the third quartiles, and the end of the upper whisker the maxima of the distributions of participants' degree of thinking modality, respectively. Distribution means are indicated by the small circles within the boxes, standard errors are indicated by the error bars starting from these circles. The means are connected with lines within each condition ($N = 60$).
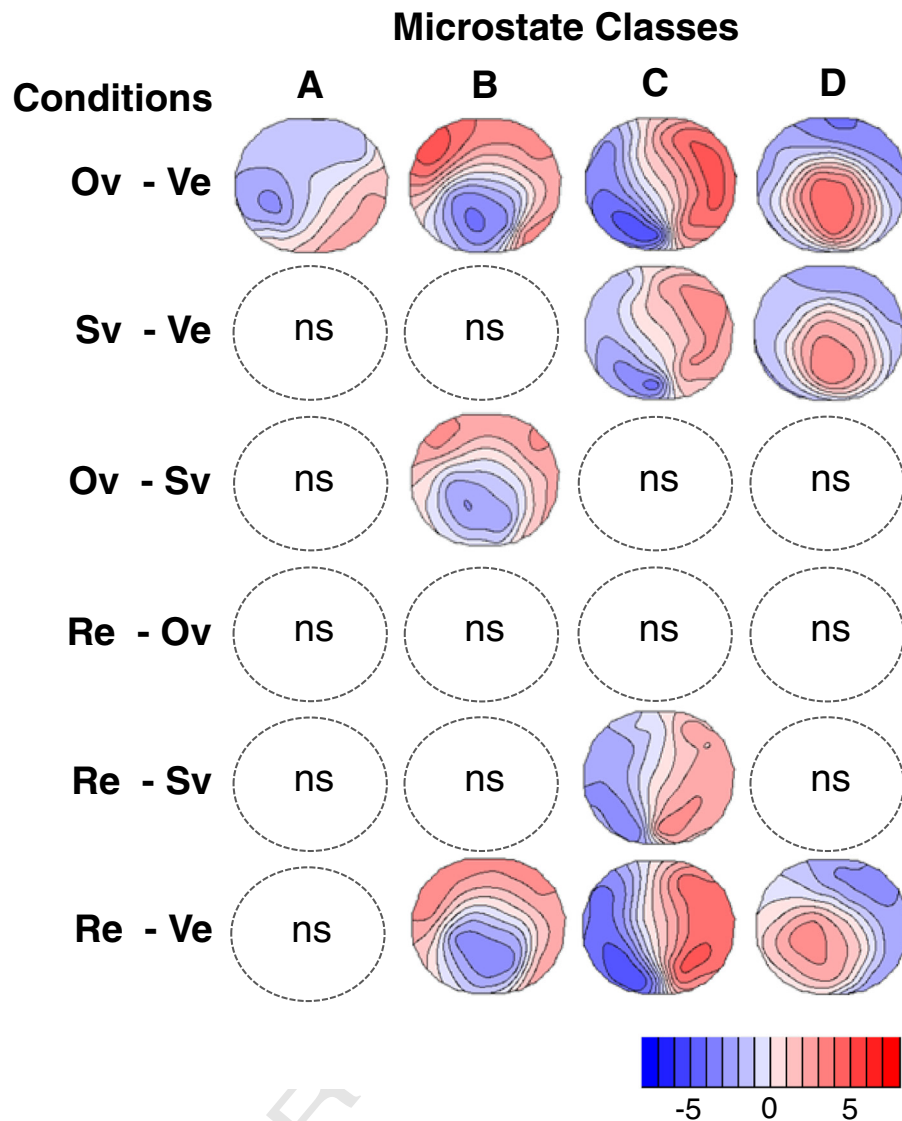
Fig. 6. Maps visualizing channel-wise paired *t*-test differences for condition pairs significantly different at $p < 0.05$ (two-tailed) for the four EEG microstate classes A, B, C, and D. Positive *t*-values are depicted in red, negative *t*-values in blue. For interpretation of the references to color in this figure legend, the reader is referred to the web version of this article.

the three tasks deviated similarly from no-task testing. Therefore, we computed the source of the mean difference between visualization (object- and spatial-visualization) and verbalization, and between tasks (object-, spatial-visualization and verbalization) and no-task resting using eLORETA (Pascual-Marqui, 2007) (Fig. 7).

During visualization compared to verbalization, source localizations revealed increased activity in left parietal areas for Map B (insula, BA 13) and Map C (temporal lobe, BA 39) and in midline posterior areas (posterior cingulate, BA23) for Map D. Increased activity during verbalization was observed in right occipito-parietal areas (posterior cingulate, BA31) for Map B, right occipito-parietal areas (insula, BA13) for Map C, and midline anterior areas (anterior cingulate, BA25) for Map D (see Fig. 6).

During tasks compared to no-task resting, source localizations revealed increased activity in left Broca's area (BA44) for Map B, the precuneus (BA7) for Map C, and the medial frontal gyrus (BA9) for Map D. Increased activity during resting was observed in the right primary somatosensory cortex (BA3) for Map B, left visual association areas (BA18) for Map C, and the left auditory association area (BA21) for Map D (see Fig. 8).

Inter-individual analysis

Pearson correlations between EEG microstate parameters across conditions revealed strong associations (all $r > 0.75$) between duration, occurrence, and coverage for all microstate classes and all condition pairs (Inline Supplementary Table S8). These results suggest that the relative duration, occurrence, and coverage of the four EEG microstate classes of the same participant compared to others are very similar during all conditions. A participant with a comparably long duration of EEG microstate class A during resting, will also exhibit a comparably long duration of microstate class A during tasks, and vice versa.

Fig. 7. eLORETA brain images of the statistical difference in cortical distribution of electric sources of the three microstate classes B, C, and D between visualization (Vis) and verbalization (Ve). Left to right: slices in axial (from top, nose up), sagittal (from left) and coronal (from back) view in MNI space. Images depict all t-values with $p < 0.05$ (two-tailed), $t = 2.00$ ($df = 60$). Red = stronger activity during visualization, blue = stronger activity during verbalization. Vis > Ve: slices through the voxel (indicated by arrowheads) of maximally stronger activity during visualization. Vis < Ve: slices through the voxel (indicated by arrowheads) of maximally stronger activity during verbalization. The MNI coordinates (X, Y, Z) of these voxels are reported in millimeters. For interpretation of the references to color in this figure legend, the reader is referred to the web version of this article.

Microstate Classes
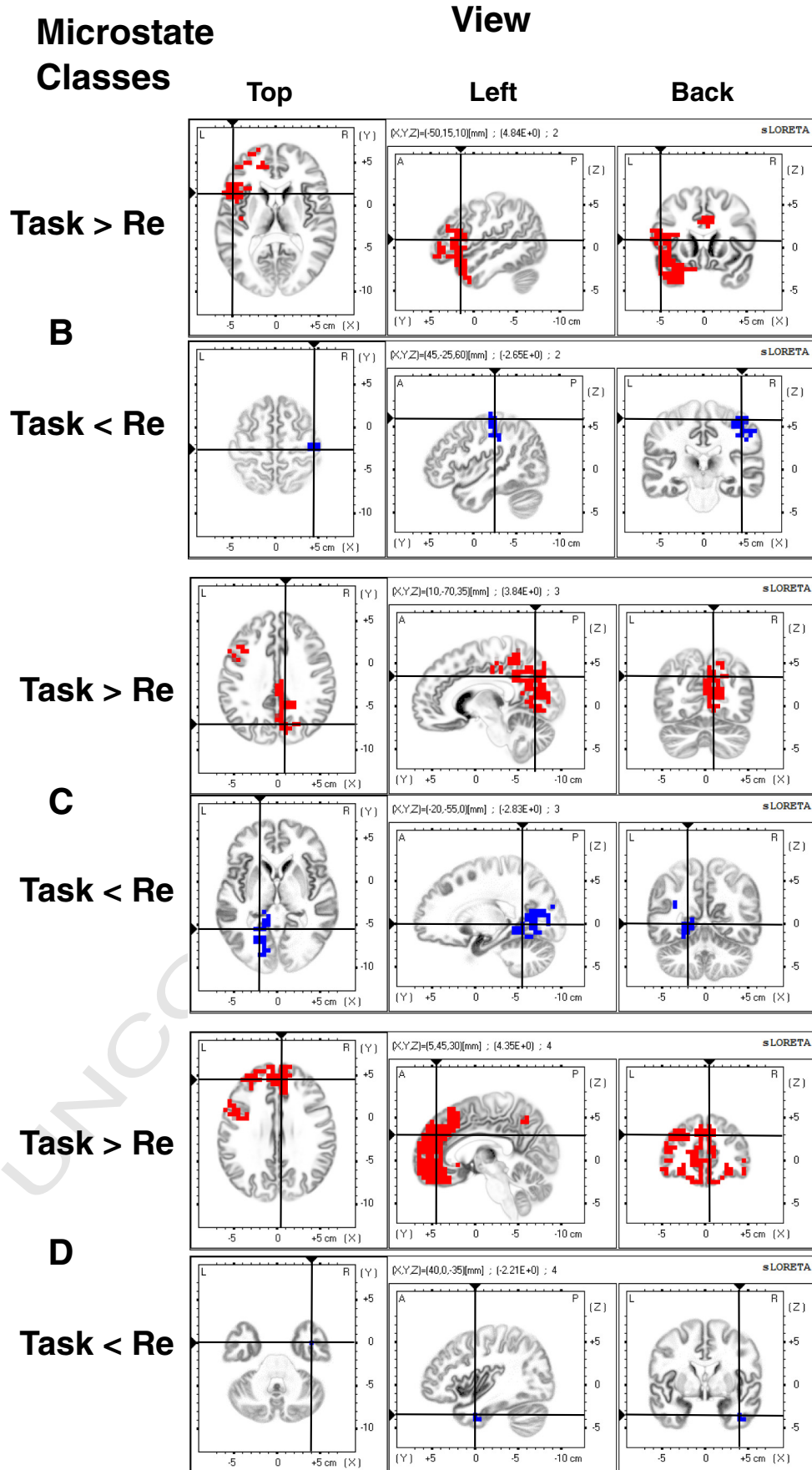
View
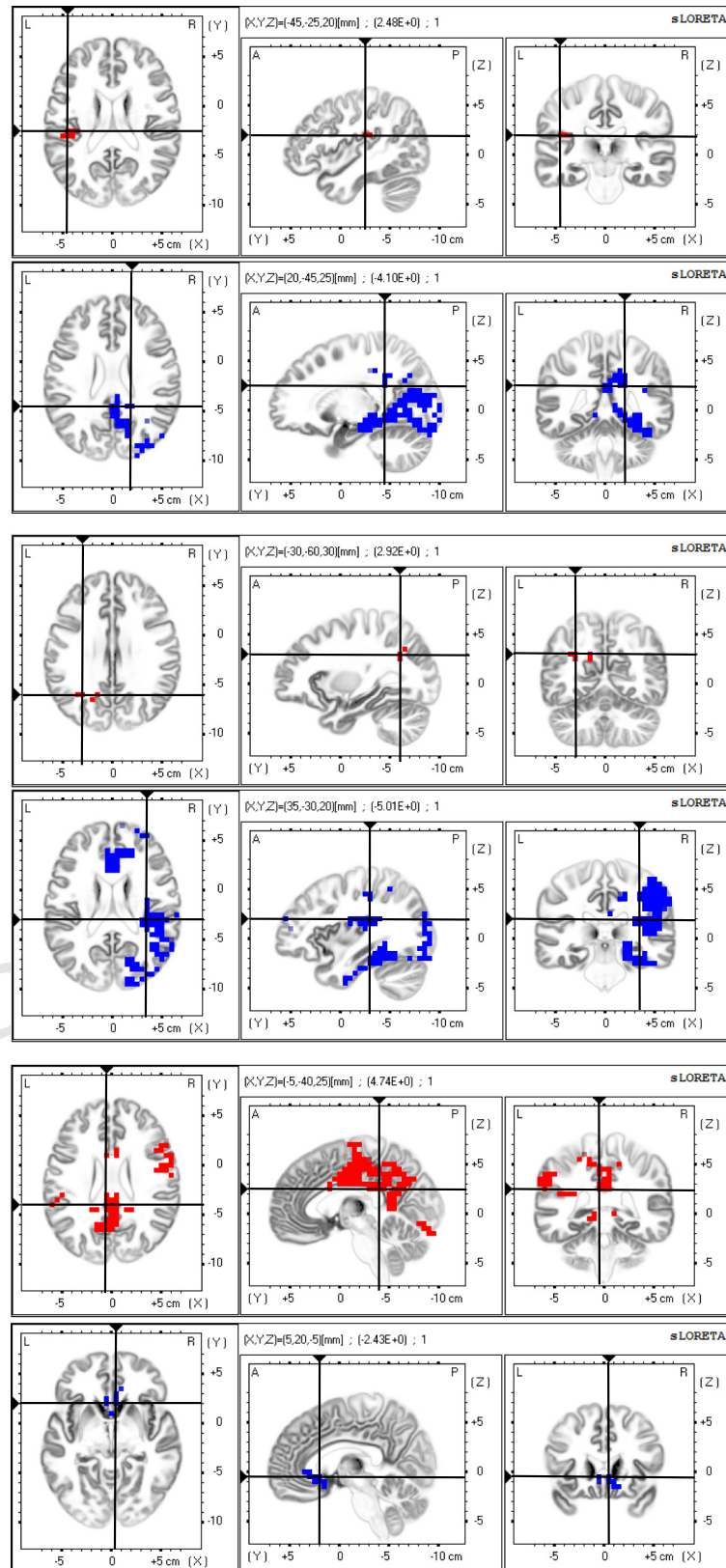
Table 7

Correlations (Pearson's r) between the microstate parameters (duration, occurrence, coverage) during no-task resting of the four EEG microstate classes (A, B, C, D) with three modality-related person parameters: modality-specific ability (Ability), modality-specific style (Style), and self-reported thinking modality (Thinking).

Microstate parameters	Modalities	Modality-related personal parameters											
		Ability				Style				Thinking			
		A	B	C	D	A	B	C	D	A	B	C	D
Duration	Object-visual	0.04	−0.03	0.07	0.06	0.07	0.20	0.10	−0.12	0.01	−0.01	***<u>0.28</u>***	−0.21
	Spatial-visual	0.08	0.05	0.01	0.00	0.17	0.06	0.08	−0.13	0.11	0.14	<u>0.25</u>	0.04
	Verbal	−0.13	0.14	0.00	−0.25	***<u>−0.34</u>***	−0.22	−0.08	−0.09	−0.05	−0.18	−0.09	−0.02
Occurrence	Object-visual	−0.14	−0.16	0.01	0.08	<u>−0.11</u>	0.07	−0.04	−0.12	−0.03	−0.11	0.21	−0.15
	Spatial-visual	−0.04	−0.01	−0.16	0.11	−0.02	−0.05	0.03	0.09	−0.11	−0.10	−0.12	−0.27
	Verbal	0.02	0.19	0.15	−0.10	0.02	0.08	***<u>0.28</u>***	0.24	0.04	0.04	0.15	0.04
Coverage	Object-visual	−0.08	−0.13	0.07	0.09	−0.07	0.19	<u>0.05</u>	−0.13	−0.02	−0.07	***<u>0.32</u>***	−0.25
	Spatial-visual	0.02	0.01	−0.08	0.05	0.05	−0.01	0.05	−0.07	−0.04	0.01	<u>0.11</u>	−0.08
	Verbal	−0.02	0.24	0.10	−0.25	−0.14	−0.05	0.11	0.04	0.04	−0.07	0.04	−0.01

R-values of significant (p < 0.05 no correction for multiple testing) correlations are highlighted in bold, italic, and underlined.

Inline Supplementary Table S8 can be found online at http://dx.doi.org/10.1016/j.neuroimage.2015.08.023.

Pearson correlations between EEG microstate classes and behavioral variables (Table 7) inspected whether these relatively stable inter-individual differences in the EEG microstate class parameter distributions might be associated with modality-related personal parameters.

However, only four of the 108 possible correlations between the three EEG microstate parameters and the three modality-related personal parameters were significant at $p < 0.05$ (not corrected for multiple testing). The first two significant correlations concerned object-visual thinking during resting. Object-visual thinking was positively associated with the duration and coverage of microstate class C. However, post-hoc run-wise analyses revealed that these significant correlations did not occur consistently across runs (Inline Supplementary Tables S9 and S10). The other two significant correlations concerned verbal cognitive style. Verbal style was negatively associated with the duration of microstate class A, and positively associated with the occurrence of microstate class C.

Inline Supplementary Tables S9 and S10 can be found online at http://dx.doi.org/10.1016/j.neuroimage.2015.08.023.

Discussion

As hypothesized, EEG microstate parameters and topographies were affected by an individual's degree of visual and verbal thinking, and differed between internal, goal-directed tasks and no-task resting.

Intra-individual differences

EEG microstate parameters

Participants' subjective ratings suggest that our tasks successfully induced object-visual, spatial-visual, and verbal thinking using three corresponding tasks. EEG microstate parameter differences between the three tasks were compared to each other and to resting. These comparisons revealed an association of microstate class A with visualization and microstate class B with verbalization. Microstate class D was associated with no-task resting, possibly reflecting the increase of the degree of subjective interoceptive-autonomic processing particular to no-task resting compared to the three goal-directed tasks.

Our results are in line with the findings of Britz et al. (2010) with regard to microstate class D. In their combined fMRI EEG study, microstate class D was also associated with subjective interoceptive-autonomic processing, namely an fMRI resting-state network that had previously been attributed to this processing mode. However, our associations of microstate classes A and B at first sight appear to conflict with their findings. Whereas we found increased duration, occurrence, and coverage of microstate class A during visualization, and of microstate class B during verbalization, Britz et al. (2010) associated microstate class A with fMRI resting-state networks that had previously been attributed to phonological processing, and microstate class B with fMRI resting-state networks previously attributed to visual imagery.

According to Pascual-Marqui et al. (2014), the four EEG microstate classes are produced by a strong common generator in the posterior cortex, with an additional generator in left occipital areas for microstate class A, right occipital areas for microstate class B, and anterior cingulate areas for microstate class C. Again our results at first sight appear to conflict with this finding. Why would we find increased duration, occurrence, and coverage of left-lateralized vs. right-lateralized microstates during visualization compared to verbalization and vice versa when in the literature language processing has primarily been associated (though clearly not uniquely, see e.g. Jonides et al., 1998) with a large-scale left-hemispheric network (Buchsbaum et al., 2001; Vigneau et al., 2006), whereas secondary visual processing has been primarily associated (though again clearly not uniquely, see e.g. Mehta and Newcombe, 1991; Sergent, 1990) with right-lateralized regions, particularly the right-posterior parietal cortex (Malhotra et al., 2009; Newcombe et al., 1987; Weiss et al., 2006)?

A possible answer to this question may be associated with the EEG frequency band range and the computation of the four EEG microstate classes is based on our knowledge of the location of their intra-cortical sources (Pascual-Marqui et al., 2014). The computation of EEG microstate topographies is conventionally performed on EEG data band-pass filtered from 2 to 20 Hz (e.g. Koenig et al., 2002; Lehmann et al., 2005; Pascual-Marqui et al., 2014). However, the frequency band with the strongest power in this frequency range is the alpha band. The functional significance of EEG alpha activity has been a matter of debate (Bazanova and Vernon, 2014). It may depend on the specific frequency range (upper vs. lower alpha) and its cortical sources. However, the primary cortical sources of the EEG microstate classes are posterior where alpha exhibits inhibitory rather than excitatory functions on modality-specific processing (Harmony, 2013; Niedermeyer and da Silva, 2005; O'gorman et al., 2013; Pfurtscheller, 2003; Pfurtscheller and Da Silva, 1999; Pfurtscheller et al., 1996). Consequently, we suggest that microstate class A with its left-posterior source is observed more frequently during visualization because it reflects activation in a left-posterior hub which triggers inhibition of the connected left-hemispheric areas

Fig. 8. eLORETA brain images of the statistical difference in cortical distribution of electric sources of the three microstate classes B, C, and D between tasks (Task) and no-task resting (Re). Left to right: slices in axial (from top, nose up), sagittal (from left) and coronal (from back) view in MNI space. Images depict all t-values with $p < 0.05$ (two-tailed), $t = 2.00$ ($df = 60$). Red = stronger activity during tasks, blue = stronger activity during no-task resting. Task > Re: slices through the voxel (indicated by arrowheads) of maximally stronger activity during tasks. Task < Re: slices through the voxel (indicated by arrowheads) of maximally stronger activity during resting. The MNI coordinates (X, Y, Z) of these voxels are reported in millimeters. For interpretation of the references to color in this figure legend, the reader is referred to the web version of this article.

related to language processing, whereas microstate class B with its right-posterior source is observed more frequently during verbalization because it reflects activation in a right-posterior hub which triggers inhibition of the connected right-hemispheric areas related to visuo-spatial processing. Studies on the effective connectivity of the brain sources of the four EEG microstates are needed to shed more light on this issue.

EEG microstate topographies

Comparing the EEG microstate topographies between the four conditions revealed significant topographic differences for microstate classes B, C, and D. These differences varied across classes. This suggests that the biological correlates of mental states representing modalities such as visual vs. verbal/abstract are themselves (micro-) state dependent, which is something that, to our knowledge, has not been taken into account previously (e.g. Koenig et al., 1998; Lehmann et al., 1998, 2010).

Intra-cortical source localizations revealed stronger left parietal (BA13, BA39) and weaker right occipito-parietal (BA31, BA13) activation for visualization compared to verbalization for microstate classes B and C respectively. These left–right topography differences for microstate classes B and C might again reflect increased inhibitory activity in left-lateralized areas of verbal processing (Buchsbaum et al., 2001; LLoyd, 2007; Vigneau et al., 2006) and decreased inhibitory activity in right-lateralized areas of spatial-visual processing (LLoyd, 2007; Malhotra et al., 2009; Newcombe et al., 1987; Weiss et al., 2006).

For microstate class D, posterior cingulate activity (BA23) was stronger and anterior cingulate (BA25) activity weaker during visualization compared to verbalization. Unlike posterior areas associated with modality-specific processing, the anterior cingulate cortex (ACC) is not primarily regarded as a source of alpha but as a source of EEG theta activity. EEG theta induced by activity in the ACC is referred to as *frontal midline theta*. This distinct rhythm occurs during working-memory tasks (Asada et al., 1999; Ishii et al., 1999) and correlates positively with demands on attention and executive processing (Gevins et al., 1997). These findings suggest that increased ACC activity during verbalization may be interpreted as increased demands on attention and executive processing compared to visualization. The interpretation of increased posterior cingulate activity during visualization is less straightforward. Its maxima was localized in an area previously associated with spatial orientation and memory (Vogt et al., 1992). However, since it extends beyond the posterior cingulate cortex to the motor- and somatosensory cortices, it may also reflect increased alpha inhibition of information processing in competing modalities. In line with this hypothesis, opposing alpha effects in visual as opposed to motor- and somatosensory cortical areas have frequently been reported (Pfurtscheller, 2003).

The areas of increased activity during no-task resting compared to the three tasks largely overlap with areas previously reported to be associated with the dorsal medial prefrontal cortex subsystem, a default mode network subsystem associated with introspection about mental states. The areas of increased activity during tasks largely overlap with areas associated with the medial temporal lobe subsystem and primary default mode network hubs which have been associated with memory-based construction/ simulation and valuation of motivationally-salient/personally-significant information respectively (Andrews-Hanna, 2012). Future studies must reveal the interplay of the cortical neuronal rhythms that these networks rely on.

Inter-individual differences

EEG microstate parameters

Pearson correlations revealed strong associations between the distributions of the three parameters of the four EEG microstate classes across conditions (all $r > 0.75$). These results suggest that beyond task-specificity, the EEG microstate parameters also exhibit strong person-specificity.

Pearson correlations between behavioral variables and EEG microstate parameters during resting revealed no consistent associations with participants' degree of object-visual, spatial-visual, and verbal thinking during resting or participants' modality-specific cognitive abilities. However, verbal cognitive style was negatively associated with the duration of microstate class A, and positively associated with the occurrence of microstate class C. The negative association with class A is in line with our observed task differences which suggest that class A duration is shortened during verbalization compared to visualization. However, due to the exploratory nature of this investigation, many correlations had to be computed and significant results (not corrected for multiple testing) only concerned singular parameter–modality pairs. Hypothesis-driven studies or studies of larger sample sizes are needed to validate our results.

The lack of associations between EEG microstate parameters with reported thinking modality and modality-specific cognitive abilities may be due to a number of reasons. Firstly, other factors such as alertness, wakefulness, and/or other personality traits (Knyazev et al., 2004; Schmidtke and Heller, 2004; Stenberg, 1992) which are known to affect EEG parameters and differ between participants may play a confounding role. Moreover, with regard to reported thinking modality, participants may struggle with reporting their degree of object-, spatial-visual, and verbal thinking with the necessary precision and similar point of reference to allow comparing these reports between individuals. Furthermore, we note that participants' reported thinking modality referred to their perception of the whole duration of the 50 s recording run. However, on average only 25.76 s of clean EEG for each run was available for analysis. This limitation of overlap between the time period rated and the time period analyzed may also contribute to the lack of consistent inter-individual associations between EEG microstate parameters and subjectively reported thinking modality.

The functional significance of the EEG microstate classes

Our inter-individual results showed clear associations of the left-lateralized microstate class A with visual, and the right-lateralized microstate class B with verbal processing. The increased duration, occurrence, and coverage of these microstate classes during the respective tasks might reflect increased inhibitory activity in default mode network hubs associated with areas associated with language and visuo-spatial processing, respectively. Complementary to this effect, topographic analyses suggested a shift of two microstate classes (B and C) towards increased left-hemispheric and decreased right-hemispheric source activity for visualization compared to verbalization. Apparently, when the same four microstate classes are enforced for visualization and verbalization conditions, the lateralization difference shows in the predominance of the two lateralized microstate classes A and B, whereas when the microstate classes for the tasks are inspected separately, microstate classes B and C appear more right- respectively left-lateralized.

Conclusions

Our results revealed associations of microstate classes A and B with visual and verbal processing respectively, and microstate class D with interoceptive-autonomic processing. However, all microstate classes occurred in all four conditions and the absolute differences of coverage for microstate classes A and B for visualization compared to verbalization conditions, and the absolute differences of coverage for microstate class D for no-task resting compared to goal-directed tasks are considerably small. Therefore, we suggest that while increased occurrence, duration, and coverage of EEG microstate classes A, B, and D can clearly be associated with visual, verbal, and interoceptive-autonomic processing respectively, they can certainly not be reduced to these functions.

Instead, a finely-tuned interplay between the four EEG microstate classes is necessary for the continuous formation of visual and verbal thoughts, as well as interoceptive-autonomic processing. Our results point to the possibility that the EEG microstate classes may represent the head-surface measured activity of intra-cortical sources primarily exhibiting inhibitory functions. However, additional studies are needed to verify and elaborate on this hypothesis.

Acknowledgments

References

Andreou, C., Faber, P.L., Leicht, G., Schoettle, D., Polomac, N., Hanganu-Opatz, I.L., Lehmann, D., Mulert, C., 2014. Resting-state connectivity in the prodromal phase of schizophrenia: insights from EEG microstates. Schizophr. Res. 152, 513–520.

Andrews-Hanna, J.R., 2012. The brain's default network and its adaptive role in internal mentation. Neuroscientist 18, 251–270.

Asada, H., Fukuda, Y., Tsunoda, S., Yamaguchi, M., Tonoike, M., 1999. Frontal midline theta rhythms reflect alternative activation of prefrontal cortex and anterior cingulate cortex in humans. Neurosci. Lett. 274, 29–32.

Baschek, I.L., Bredenkamp, J., Oehrle, B., Wippich, W., 1977. Assessment of imagery (I), concreteness (C) and meaningfulness (m1) of 800 nouns. Z. Exp. Angew. Psychol. 24, 353–396.

Bazanova, O.M., Vernon, D., 2014. Interpreting EEG alpha activity. Neurosci. Biobehav. Rev. 44, 94–110.

Becker, D., Creutzfeldt, O., Schwibbe, M., Wuttke, W., 1982. Changes in physiological, EEG and psychological parameters in women during the spontaneous menstrual cycle and following oral contraceptives. Psychoneuroendocrinology 7, 75–90.

Blazhenkova, O., Kozhevnikov, M., 2009. The new object-spatial-verbal cognitive style model: theory and measurement. Appl. Cogn. Psychol. 23, 638–663.

Britz, J., Van De Ville, D., Michel, C.M., 2010. BOLD correlates of EEG topography reveal rapid resting-state network dynamics. NeuroImage 52, 1162–1170.

Brodbeck, V., Kuhn, A., von Wegner, F., Morzelewski, A., Tagliazucchi, E., Borisov, S., Michel, C.M., Laufs, H., 2012. EEG microstates of wakefulness and NREM sleep. NeuroImage 62, 2129–2139.

Buchsbaum, B.R., Hickok, G., Humphries, C., 2001. Role of left posterior superior temporal gyrus in phonological processing for speech perception and production. Cogn. Sci. 25, 663–678.

Chatrian, G., Lettich, E., Nelson, P., 1985. Ten percent electrode system for topographic studies of spontaneous and evoked EEG activities. Am. J. EEG Technol. 25, 83–92.

Ekstrom, R.B., French, J.W., Harman, H.H., Derman, D., 1976. Manual for kit of factor-referenced cognitive tests. Educational Testing Service, Princeton, NJ.

Faber, P.L., Lehmann, D., Barendregt, H., Kaelin, M., Gianotti, L.R., 2005. Increased duration of EEG microstates during meditation. Brain Topogr. 18, 131.

Faber, P., Lehmann, D., Milz, P., Travis, F., Parim, N., 2014. EEG microstates differ between transcending and mind wandering. ZNZ Symposium 2014, Zurich.

Fingelkurts, A.A., Fingelkurts, A.A., Bagnato, S., Boccagni, C., Galardi, G., 2012. EEG oscillatory states as neuro-phenomenology of consciousness as revealed from patients in vegetative and minimally conscious states. Conscious. Cogn. 21, 149–169.

Gevins, A., Smith, M.E., McEvoy, L., Yu, D., 1997. High-resolution EEG mapping of cortical activation related to working memory: effects of task difficulty, type of processing, and practice. Cereb. Cortex 7, 374–385.

Harmony, T., 2013. The functional significance of delta oscillations in cognitive processing. Front. Integr. Neurosci. 7.

Horn, W., 1962. Leistungsprüfsystem, LPS: Handanweisung für die Durchführung, Auswertung und Interpretation.

IBM Corporation, 2014. IBM SPSS Statistics for Windows, Version 22.0. IBM Corp., Armonk, NY.

Ishii, R., Shinosaki, K., Ukai, S., Inouye, T., Ishihara, T., Yoshimine, T., Hirabuki, N., Asada, H., Kihara, T., Robinson, S.E., Takeda, M., 1999. Medial prefrontal cortex generates frontal midline theta rhythm. Neuroreport 10, 675–679.

Jäger, A.O., Süß, H.-M., Beauducel, A., 1997. Berliner Intelligenzstruktur-Test, BIS-Test. Form 4. Handanweisung (The Berlin Intelligence Structure Test, BIS test. 4. Form. Test Manual). Hogrefe, Göttingen.

Jonides, J., Schumacher, E.H., Smith, E.E., Koeppe, R.A., Awh, E., Reuter-Lorenz, P.A., Marshuetz, C., Willis, C.R., 1998. The role of parietal cortex in verbal working memory. J. Neurosci. 18, 5026–5034.

Katayama, H., Gianotti, L.R., Isotani, T., Faber, P.L., Sasada, K., Kinoshita, T., Lehmann, D., 2007. Classes of multichannel EEG microstates in light and deep hypnotic conditions. Brain Topogr. 20, 7–14.

Kikuchi, M., Koenig, T., Wada, Y., Higashima, M., Koshino, Y., Strik, W., Dierks, T., 2007. Native EEG and treatment effects in neuroleptic-naive schizophrenic patients: time and frequency domain approaches. Schizophr. Res. 97, 163–172.

Kindler, J., Hubl, D., Strik, W., Dierks, T., Koenig, T., 2011. Resting-state EEG in schizophrenia: auditory verbal hallucinations are related to shortening of specific microstates. Clin. Neurophysiol. 122, 1179–1182.

Knyazev, G.G., Savostyanov, A.N., Levin, E.A., 2004. Alpha oscillations as a correlate of trait anxiety. Int. J. Psychophysiol. 53, 147–160.

Koenig, T., Kochi, K., Lehmann, D., 1998. Event-related electric microstates of the brain differ between words with visual and abstract meaning. Electroencephalogr. Clin. Neurophysiol. 106, 535–546.

Koenig, T., Lehmann, D., Merlo, M.C., Kochi, K., Hell, D., Koukkou, M., 1999. A deviant EEG brain microstate in acute, neuroleptic-naive schizophrenics at rest. Eur. Arch. Psychiatry Clin. Neurosci. 249, 205–211.

Koenig, T., Prichep, L., Lehmann, D., Sosa, P.V., Braeker, E., Kleinlogel, H., Isenhart, R., John, E.R., 2002. Millisecond by millisecond, year by year: normative EEG microstates and developmental stages. NeuroImage 16, 41–48.

Koenig, T., Kottlow, M., Stein, M., Melie-García, L., 2011. Ragu: a free tool for the analysis of EEG and MEG event-related scalp field data using global randomization statistics. Comput. Intell. Neurosci. 2011, 4.

Krug, R., Moelle, M., Fehm, H., Born, J., 1999. Variations across the menstrual cycle in EEG activity during thinking and mental relaxation. J. Psychophysiol. 13, 163–172.

Lehmann, D., 1990. Brain electric microstates and cognition: the atoms of thought. Machinery of the Mind. Springer, pp. 209–224.

Lehmann, D., Michel, C.M., 2011. EEG-defined functional microstates as basic building blocks of mental processes. Clin. Neurophysiol. 122, 1073–1074.

Lehmann, D., Skrandies, W., 1980. Reference-free identification of components of checkerboard-evoked multichannel potential fields. Electroencephalogr. Clin. Neurophysiol. 48, 609–621.

Lehmann, D., Ozaki, H., Pal, I., 1987. EEG alpha map series: brain micro-states by space-oriented adaptive segmentation. Electroencephalogr. Clin. Neurophysiol. 67, 271–288.

Lehmann, D., Strik, W., Henggeler, B., Koenig, T., Koukkou, M., 1998. Brain electric microstates and momentary conscious mind states as building blocks of spontaneous thinking: I. Visual imagery and abstract thoughts. Int. J. Psychophysiol. 29, 1–11.

Lehmann, D., Koenig, T., Henggeler, B., Strik, W., Kochi, K., Koukkou, M., Pascual-Marqui, R., 2004. Brain areas activated during electric microstates of mental imagery versus abstract thinking. Klin. Neurophysiol. 35, 160.

Lehmann, D., Faber, P.L., Galderisi, S., Herrmann, W.M., Kinoshita, T., Koukkou, M., Mucci, A., Pascual-Marqui, R.D., Saito, N., Wackermann, J., 2005. EEG microstate duration and syntax in acute, medication-naive, first-episode schizophrenia: a multi-center study. Psychiatry Res. Neuroimaging 138, 141–156.

Lehmann, D., Pascual-Marqui, R.D., Michel, C., 2009. EEG microstates. Scholarpedia 4, 7632.

Lehmann, D., Pascual-Marqui, R.D., Strik, W.K., Koenig, T., 2010. Core networks for visual-concrete and abstract thought content: a brain electric microstate analysis. NeuroImage 49, 1073–1079.

LLoyd, D., 2007. "What Do Brodmann Areas Do?," Or: Scanning the Neurocracy. CT: Program in Neuroscience, Hartford.

Malhotra, P., Coulthard, E.J., Husain, M., 2009. Role of right posterior parietal cortex in maintaining attention to spatial locations over time. Brain awn350.

Marks, D.F., 1973. Visual imagery differences in the recall of pictures. Br. J. Psychol. 64, 17–24.

Mehta, Z., Newcombe, F., 1991. A role for the left hemisphere in spatial processing. Cortex 27, 153–167.

Meili, R., 1955. Würfelabwicklungen. Huber, Bern.

Michel, C., Brandeis, D., Koenig, T., 2009. Electrical neuroimaging in the time domain. In: Michel, C., Koenig, T., Brandeis, D., Gianotti, L., Wackermann, J. (Eds.), Electrical Neuroimaging. Cambridge University Press, Cambridge, pp. 111–143.

Milz, P., 2015n. The KEY EEG Python Library: keypy (in preparation for upload to public github repository). **Q17**

Milz, P., Faber, P., Lehmann, D., 2015. The Modality of Thinking Questionnaire—A New Self-Report Measure of Object-Spatial–Verbal Cognitive Style (submitted for publication). **Q18**

Newcombe, F., Ratcliff, G., Damasio, H., 1987. Dissociable visual and spatial impairments following right posterior cerebral lesions: clinical, neuropsychological and anatomical evidence. Neuropsychologia 25, 149–161.

Niedermeyer, E., da Silva, F.L., 2005. Electroencephalography: basic principles, clinical applications, and related fields. Lippincott Williams & Wilkins.

Nishida, K., Morishima, Y., Yoshimura, M., Isotani, T., Irisawa, S., Jann, K., Dierks, T., Strik, W., Kinoshita, T., Koenig, T., 2013. EEG microstates associated with salience and frontoparietal networks in frontotemporal dementia, schizophrenia and Alzheimer's disease. Clin. Neurophysiol. 124, 1106–1114.

Nuwer, M.R., 1987. Recording electrode site nomenclature. J. Clin. Neurophysiol. 4, 121–133.

O'gorman, R., Poil, S.-S., Brandeis, D., Klaver, P., Bollmann, S., Ghisleni, C., Lüchinger, R., Martin, E., Shankaranarayanan, A., Alsop, D., 2013. Coupling between resting cerebral perfusion and EEG. Brain Topogr. 26, 442–457.

Oldfield, R.C., 1971. The assessment and analysis of handedness: the Edinburgh inventory. Neuropsychologia 9, 97–113.

Pascual-Marqui, R.D., 2007. Discrete, 3D distributed, linear imaging methods of electric neuronal activity. Part 1: exact, zero error localization (arXiv preprint arXiv: 0710.3341).

Pascual-Marqui, R.D., Michel, C.M., Lehmann, D., 1995. Segmentation of brain electrical activity into microstates: model estimation and validation. IEEE Trans. Biomed. Eng. 42, 658–665.

Pascual-Marqui, R.D., Lehmann, D., Faber, P., Milz, P., Kochi, K., Yoshimura, M., Nishida, K., Isotani, T., Kinoshita, T., 2014. The resting microstate networks (RMN): cortical distributions, dynamics, and frequency specific information flow (arXiv preprint arXiv: 1411.1949).

Pfurtscheller, G., 2003. Induced oscillations in the alpha band: functional meaning. Epilepsia 44, 2–8.

Pfurtscheller, G., Da Silva, F.L., 1999. Event-related EEG/MEG synchronization and desynchronization: basic principles. Clin. Neurophysiol. 110, 1842–1857.

948 Pfurtscheller, G., Stancak, A., Neuper, C., 1996. Event-related synchronization (ERS) in the
949   alpha band—an electrophysiological correlate of cortical idling: a review. Int.
950   J. Psychophysiol. 24, 39–46.
951 Schlegel, F., Lehmann, D., Faber, P.L., Milz, P., Gianotti, L.R., 2012. EEG microstates during
952   resting represent personality differences. Brain Topogr. 25, 20–26.
953 Schmidtke, J.I., Heller, W., 2004. Personality, affect and EEG: predicting patterns of region-
954   al brain activity related to extraversion and neuroticism. Personal. Individ. Differ. 36,
955   717–732.
956 Sergent, J., 1990. The neuropsychology of visual image generation: data, method, and the-
957   ory. Brain Cogn. 13, 98–129.
958 Stenberg, G., 1992. Personality and the EEG: arousal and emotional arousability. Personal.
959   Individ. Differ. 13, 1097–1113.
960 Strelets, V., Faber, P., Golikova, J., Novototsky-Vlasov, V., Koenig, T., Gianotti, L, Gruzelier,
961   J., Lehmann, D., 2003. Chronic schizophrenics with positive symptomatology have
962   shortened EEG microstate durations. Clin. Neurophysiol. 114, 2043–2051.
963 Strik, W., Dierks, T., Becker, T., Lehmann, D., 1995. Larger topographical variance and de-
964   creased duration of brain electric microstates in depression. J. Neural Transm. Gen.
965   Sect. JNT 99, 213–222.
966 Strik, W.K., Chiaramonti, R., Muscas, G.C., Paganini, M., Mueller, T.J., Fallgatter, A.J., Versari,
967   A., Zappoli, R., 1997. Decreased EEG microstate duration and anteriorisation of the
968   brain electrical fields in mild and moderate dementia of the Alzheimer type. Psychi-
969   atry Res. Neuroimaging 75, 183–191.
970 Strik, W., Fallgatter, A., Brandeis, D., Pascual-Marqui, R., 1998. Three-dimensional tomog-
971   raphy of event-related potentials during response inhibition: evidence for phasic
972   frontal lobe activation. Electroencephalogr. Clin. Neurophysiol. Evoked Potentials
973   Sect. 108, 406–413.
998

974 Tomescu, M.I., Rihs, T.A., Becker, R., Britz, J., Custo, A., Grouiller, F., Schneider, M., Debbané,
975   M., Eliez, S., Michel, C.M., 2014. Deviant dynamics of EEG resting state pattern in
976   22q11.2 deletion syndrome adolescents: a vulnerability marker of schizophrenia?
977   Schizophr. Res. 157, 175–181.
978 Tomescu, M.I., Rihs, T.A., Roinishvili, M., Karahanoglu, F.I., Schneider, M., Menghetti, S.,
979   Van De Ville, D., Brand, A., Chkonia, E., Eliez, S., Herzog, M.H., Michel, C.M., Cappe,
980   C., 2015. Schizophrenia patients and 22q11.2 deletion syndrome adolescents at risk
981   express the same deviant patterns of resting state EEG microstates: a candidate
     endophenotype of schizophrenia. Schizophr. Res. Cogn.   **Q16**
983 Vigneau, M., Beaucousin, V., Herve, P.-Y., Duffau, H., Crivello, F., Houde, O., Mazoyer, B.,
984   Tzourio-Mazoyer, N., 2006. Meta-analyzing left hemisphere language areas: phonol-
985   ogy, semantics, and sentence processing. NeuroImage 30, 1414–1432.
986 Vogt, B.A., Finch, D.M., Olson, C.R., 1992. Functional heterogeneity in cingulate cortex: the
987   anterior executive and posterior evaluative regions. Cereb. Cortex 2, 435–443.
988 Wackermann, J., Lehmann, D., Michel, C., Strik, W., 1993. Adaptive segmentation of spon-
989   taneous EEG map series into spatially defined microstates. Int. J. Psychophysiol. 14,
990   269–283.
991 Wehrle, R., Kaufmann, C., Wetter, T.C., Holsboer, F., Auer, D.P., Pollmächer, T., Czisch, M.,
992   2007. Functional microstates within human REM sleep: first evidence from fMRI of
993   a thalamocortical network specific for phasic REM periods. Eur. J. Neurosci. 25,
994   863–871.
995 Weiss, P.H., Rahbari, N.N., Lux, S., Pietrzyk, U., Noth, J., Fink, G.R., 2006. Processing the spa-
996   tial configuration of complex actions involves right posterior parietal cortex: an fMRI
997   study with clinical implications. Hum. Brain Mapp. 27, 1004–1014.